ELSEVIER

Catalysis Today 46 (1998) 155–163

CATALYSIS TODAY

# Formal treatment of catalytic combustion and catalytic conversion of methane

Olaf Deutschmann*, Frank Behrendt, Jürgen Warnatz

*Interdisciplinary Center of Scientific Computing, Heidelberg University, Im Neuenheimer Feld 368, D-69120, Heidelberg, Germany*

**Abstract**

Catalytic combustion and conversion of methane is investigated numerically for transient one-dimensional flow configurations (catalytic foil and catalytic wire). The reactive flow is coupled with the processes at the gas–surface interface. The analyses include detailed reaction mechanisms in the gas phase and on the surface as well as a detailed transport model. Computational tools are applied to study the ignition of heterogeneous methane oxidation on a platinum foil and the transition from heterogeneous to homogeneous combustion in this system. Furthermore, the interaction of gas phase and surface reactions in catalytic conversion of methane is considered. Time-dependent selectivity and conversion are calculated. 

*Keywords:* Catalytic combustion; Catalytic conversion; Methane

## 1. Introduction

Catalytic combustion and catalytic conversion of methane have received extensive experimental and theoretical attention in the last years because of their potential to reduce pollutant emissions and to synthesize useful chemicals. The description of such heterogeneous processes requires the coupling of reactive flow with the catalytic surface. Therefore, computational tools were developed recently that provide opportunities to analyse the elementary chemical processes occurring at the gas–surface interface and couple them to the surrounding gas phase. In contrast to previous simulations [1,2], the new numerical codes are also able to compute transient problems. The aim is to achieve a quantitative understanding of catalytic combustion and conversion.

Here, the numerical simulation is applied to the catalytic combustion of methane–air mixtures flowing on a platinum foil that is heated resistively. The heterogeneous ignition is considered and explained by elementary steps occurring at the gas–surface interface. If the catalyst temperature is increased after catalytic ignition by further heating, the formation of a flame in front of the catalytic foil is observed experimentally. This transition from heterogeneous to homogeneous combustion is simulated.

The oxidative coupling of methane in the presence of catalyst is usually carried out at temperatures over 900 K. Hence, a complex interaction between heterogeneous and homogeneous reactions occurs and, besides the $C_2$-hydrocarbons, by-products like $H_2O$, CO, $CO_2$, and $H_2$ are formed. Here, the catalytic conversion of methane is modelled using different surface reaction models and coupling them to the surrounding reactive flow. Selectivity and

*Corresponding author.

0920-5861/98/$ – see front matter 
PII: S0920-5861(98)00337-X

conversion are calculated as a function of time to investigate the influence of gas phase and surface kinetics.

## 2. Numerical model

Two simple configurations particularly amenable to experiment and simulation were modelled: the stagnation flow field over a catalytic active foil and a chemical reactor containing a catalytically active wire as shown in Fig. 1. Here, the reactive flow has to be coupled with heterogeneous chemical and transport processes at the catalytic surface. The mathematical models are based on the numerical solution of the governing equations in their one-dimensional form, considering the geometry of the problem. The independent variables are time and distance normal to the catalytic surface.

In the stagnation flow configuration, a flow with uniform velocity distribution is imposed at a certain distance from the flat foil. By confining the attention to the center of this foil, edge effects can be neglected, permitting use of the one-dimensional analysis of the Navier–Stokes equations describing this system [1]. The dependent variables are density, momentum, temperature, and mass fraction of each gas phase species. These variables are independent of the radius ($r$) and depend only on the distance from the foil ($x$) and time. This system is closed by the ideal gas law. This boundary-value problem is solved as stated by Evans and Greif [3] and Kee et al. [4].

For the wire configuration, a cylindrical computational domain around the wire (placed along the cylindrical axis) is used. The governing equations are used in their one-dimensional form (cylindrical coordinates, independent of $z$-axis), where only the distance from the wire ($r$) and time are the independent variables [5,6].

The state of the catalytic surface is described by its time-dependent mean temperature and mean coverage with adsorbed species. Balance equations are established to couple the surface processes with the reactive flow. The species mass fractions ($Y_i$) at the gas–surface interface are determined by a mass balance considering diffusive ($\boldsymbol{j}_i$) and convective ($\boldsymbol{u}$) mass transport as well as the creation or depletion rate of species by gas phase ($\dot{\omega}_i$) and surface reactions ($\dot{s}_i$):

$$\int \rho \frac{\partial Y_i}{\partial t}\,\mathrm{d}V_{\mathrm{gas}} = -\int (\boldsymbol{j}_i + \rho Y_i \boldsymbol{u})\boldsymbol{n}\,\mathrm{d}A + \int \dot{s}_i M_i\,\mathrm{d}A + \int \dot{\omega}_i M_i\,\mathrm{d}V_{\mathrm{gas}} \quad (i = 1, \ldots, N_{\mathrm{g}})$$

where $\rho$ is the gas density, $M_i$ the molar mass of the species $i$, $A$ the active catalytic surface area, $V_{\mathrm{gas}}$ the gas phase control volume adjacent to the surface and $N_{\mathrm{g}}$ the number of gas phase species. The so-called Stefan velocity ($\boldsymbol{u}$) occurs at the catalytic surface

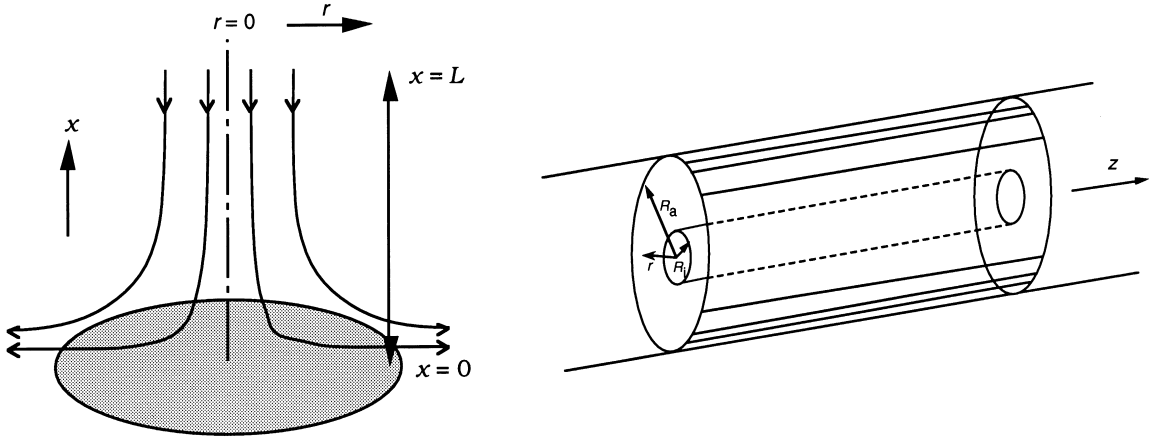


Fig. 1. Model of a stagnation flow over a foil (left) and model of a cylindrical chemical reactor ($R_a$) containing a catalytic wire ($R_i$) at its centerline (right).

if there is a net mass flux between the surface and the gas:

$$\boldsymbol{nu} = \frac{1}{\rho}\sum_{i=1}^{N_g} \dot{s}_i M_i$$

where $\boldsymbol{n}$ is the outward-pointing unit vector normal to the surface.

The temperature ($T$) of the catalyst is derived from various contributions to the energy balance at the gas–surface interface. The conductive, convective and diffusive energy transport from/to the gas phase adjacent to the surface as well as the chemical heat release, thermal radiation and external energy sources (e.g., resistive heating of the catalyst) are included. This results in

$$\begin{aligned}\int \rho c_p \frac{\partial T}{\partial t}\,\mathrm{d}V_{\mathrm{gas}} + \int \rho_{\mathrm{cat}} c_{\mathrm{cat}} \frac{\partial T}{\partial t}\,\mathrm{d}V_{\mathrm{cat}} \\ = \int \lambda \frac{\partial T}{\partial \boldsymbol{r}}\,\mathrm{d}A - \sum_{i=1}^{N_g}\int h_i(\boldsymbol{j}_i + \rho Y_i \boldsymbol{u})\boldsymbol{n}\,\mathrm{d}A \\ - \int \sigma\varepsilon\left(T^4 - T_{\mathrm{ref}}^4\right)\mathrm{d}A - \sum_{i=N_g+1}^{N_g+N_s}\int \dot{s} M_i h_i\,\mathrm{d}A \\ - \sum_{i=1}^{N_g}\int \dot{\omega}_i M_i h_i\,\mathrm{d}V_{\mathrm{gas}} + Q_{\mathrm{ext}}\end{aligned}$$

where $c_p$ is the specific heat capacity of the gas, $c_{\mathrm{cat}}$ the specific heat capacity of the catalyst, $\rho_{\mathrm{cat}}$ the density of the catalyst, $\lambda$ the thermal conductivity, $\sigma$ the Stefan–Boltzmann constant, $\varepsilon$ the surface emissivity (dependent on temperature), $T_{\mathrm{ref}}$ the reference temperature to which the surface radiates, $h_i$ the specific enthalpy of species $i$, and $Q_{\mathrm{ext}}$ the external energy source (e.g., $I^2R$ for resistive heating of the catalyst). $N_s$ is the number of surface species and $V_{\mathrm{cat}}$ is the catalyst control volume included in the energy balance.

The variation of the surface coverage ($\Theta_i$), that is, the fraction of surface sites covered by species $i$, is calculated from surface reaction rates according to

$$\frac{\partial \Theta_i}{\partial t} = \frac{\dot{s}_i}{\Gamma} \quad (i = N_g + 1, \ldots, N_g + N_s)$$

where $\Gamma$ is the surface site density of the catalyst.

A simplified multi-component transport model including thermal diffusivity is included in the governing equations. The diffusive mass flow is calculated by

$$\boldsymbol{j}_i = -\rho \frac{Y_i}{X_i} D_{i,M}\,\mathrm{grad}\,X_i - \frac{D_i^{\mathrm{T}}}{T}\,\mathrm{grad}\,T$$

where $X_i$ is the mole fraction of species $i$, $D_{i,\mathrm{M}}$ the effective diffusion coefficient of species $i$ in the mixture, and $D_i^{\mathrm{T}}$ the thermal diffusion coefficient of species $i$.

The chemistry is modelled by a set of elementary reactions in the gas phase and on the surface as well. For gas phase reactions, the temperature dependence of the rate coefficient of forward reaction $k$ is described by a modified Arrhenius expression:

$$k_{\mathrm{f}_k} = A_k\, T^{\beta_k} \exp\left[\frac{-E_{a_k}}{RT}\right]$$

For reversible reactions, the reverse rate coefficients are calculated by the equilibrium constant using thermodynamic data.

The chemical processes on the surface are treated by a formalism very similar to that for gas phase reactions by resolution into elementary reactions [7,8]. The production rate ($\dot{s}_i$) for each species is written as

$$\dot{s}_i = \sum_{k=1}^{K_s} \nu_{ik} k_{f_k} \prod_{i=1}^{N_g+N_s} [X_i]^{\nu'_{ik}}$$

Here, $K_s$ is total number of elementary surface reactions (including adsorption and desorption), $\nu_{ik}$, $\nu'_{ik}$ the stoichiometric coefficients (right minus left side of reaction equation, left side), $k_{f_k}$ the forward rate coefficient, and $[X_i]$ represents the concentration of species $i$. For adsorbed species, the concentration are given in (mol m$^{-2}$). The problem here is to find proper reaction rate coefficients. Furthermore, the rate coefficients of adsorption, desorption, and surface reactions can also depend on surface coverage. This coverage dependence is taken into account by an additional factor leading to the following rate expression for the rate coefficient of the forward reaction $k$:

$$k_{\mathrm{f}_k} = A_k T^{\beta_k} \exp\left[\frac{-E_{a_k}}{RT}\right] \prod_{i=1}^{N_s} \Theta_i^{\mu_{i_k}} \exp\left[\frac{\epsilon_{i_k}\Theta_i}{RT}\right]$$

Here, the factor $\Theta^{\mu}$ has to be considered in connection with the factor $[X]^{\nu}$ in the equation for $\dot{s}_i$.

The numerical solution of the resulting partial differential equation system is performed by the

method of lines. Spatial discretization using finite differences on statically adapted grids leads to large systems of ordinary differential and algebraic equations. These systems of coupled equations are solved by an implicit extrapolation method using the software package LIMEX [9]. The codes compute species mass fractions, temperature, and velocity (in the stagnation flow case) profiles in the gas phase, fluxes at the gas–surface interface, and surface temperature and coverage as a function of time. Since the codes are fully time-dependent, transient phenomena like ignition, oscillation, extinction or catalyst poisoning can be described.

## 3. Catalytic combustion of methane

The heterogeneous and homogeneous oxidation of methane in a stagnation point flow configuration is studied as an example of the catalytic combustion of methane. $CH_4$–air mixtures flow slowly at atmospheric pressure onto a platinum foil heated resistively. The initial gas is at room temperature and the inlet velocity is 10.9 cm $s^{-1}$ at a distance of 6.1 cm from the catalytic foil. This corresponds to a volumetric flow of 7 slpm (standard litre per minute). The foil temperature is increased stepwise by supplying electric power to the foil. When reaching the catalytic ignition temperature (depending on $CH_4$–air ratio), the temperature of the catalyst rises rapidly due to heat release by the exothermic surface reactions. Details of the experimental setup and procedure can be found elsewhere [10].

Using the computational tools, which simulate the stagnation flow field, the transient behaviour during catalytic ignition is considered. The gas phase reaction scheme is taken from modelling work of homogeneous reactive flow including reactions of the $C_1$ and $C_2$ species [11,12]. The surface reaction scheme is based on studies of catalytic methane oxidation and involves 10 surface species and 26 surface reactions [2,13]. The kinetic data used in the present study are taken from recent simulations of catalytic ignition of nitrogen-diluted $CH_4$–$O_2$ mixtures on platinum [14].

The transient numerical code offers an insight into the time-dependent behaviour of surface coverage and temperature during ignition. Fig. 2 shows the surface properties for a stoichiometric $CH_4$–air mixture after

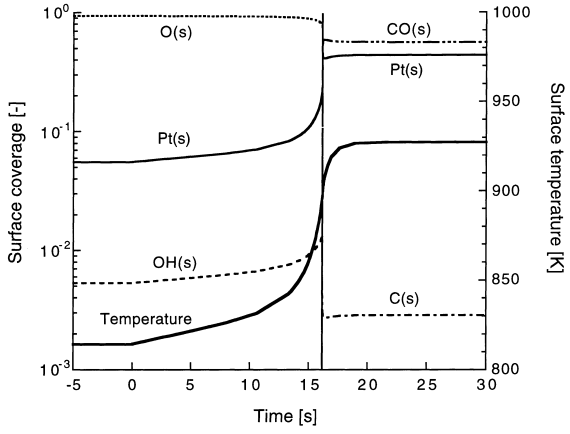


Fig. 2. Calculated time-dependent surface coverage and surface temperature of the platinum foil during heterogeneous ignition of a stoichiometric $CH_4$–air mixture. The time is zero at the final increase of electric current before ignition.

the foil is heated up to 815 K. The time scale is zero at the time of the last current increase before ignition takes place. The Pt surface is mainly covered by oxygen (O(s)) indicating that recombinative loss of oxygen must occur before methane can be adsorbed to initiate the ignition process. The global process is limited by the availability of uncovered surface sites (Pt(s)) before ignition. When the chemical heat, released by surface reactions, exceeds a critical value, the reaction becomes self-accelerating (ignition) and develops into a new stationary state controlled by mass transport. This transition occurs at $t = 16\ s$ in Fig. 2. After ignition, a sufficient number of free surface sites (Pt(s)) is available for adsorption of methane and oxygen, and the global process is controlled by diffusion of reactants toward the catalyst and products away from the catalyst. Fig. 3 clearly shows this mass transport effect. Strong gradients of the gas phase mole fraction of methane develop during ignition and the methane concentration is almost zero at the catalyst.

The experimentally observed increase of ignition temperature with decreasing methane–air ratio [10,15] is explained by the oxygen blocking before ignition [14]. A prerequisite for ignition is that the uncovered surface area (Pt(s)) is large enough to achieve adsorption rates of oxygen as well as methane molecules which give a high enough methane oxidation rate. Before ignition, the surface is mainly covered by

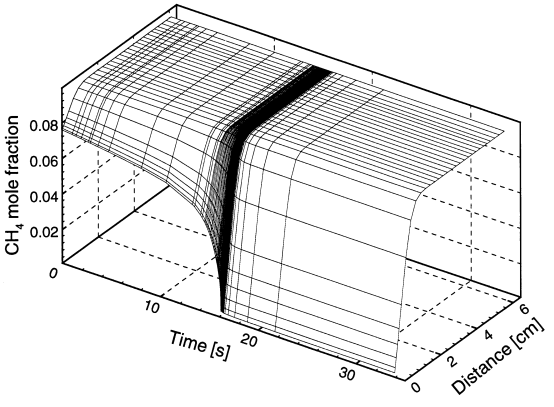


Fig. 3. Calculated methane mole fraction in the gas phase as a function of time and distance from the catalytic foil ($x$) during heterogeneous ignition of a stoichiometric $CH_4$–air mixture on a platinum foil. The time is zero at the final increase of electric current before ignition. The figure corresponds to Fig. 2.

oxygen as discussed above. Since the adsorption rate depends on the gas phase concentration, higher oxygen concentrations in the gas phase lead to larger oxygen coverage and fewer uncovered surface sites at a given temperature. Consequently, the temperature must be increased to reach the number of uncovered surface sites which is necessary for ignition. Therefore, the ignition temperature increases with decreasing methane–oxygen ratio.

A further increase in foil temperature after catalytic ignition, by a rise of electrical power applied to the foil, leads finally to homogeneous ignition. The formation of a stable flame in front of the catalyst can be observed experimentally [16]. The numerical simulation of this transition from heterogeneous to homogeneous combustion is shown in Fig. 4; the transition starts at 1.2 s. The strong gradient of the methane mole fraction shifts from the catalyst into the gas phase where the flame is formed, as shown in Fig. 4(a). For the lean mixture ($p_{CH_4}/p_{air} = 0.07$) discussed here methane is completely consumed in the flame. Fig. 4(b) reveals the stepwise temperature increase in the flame zone. Here, only the hot exhaust gases flow on the catalytic foil where thermal radiation leads to a lower temperature in comparison to that of the flame.

The calculated ignition temperatures (catalytic; 815 K for a stoichiometric mixture, homogeneous: 1300 K for a lean mixture with $p_{CH_4}/p_{air} = 0.07$) agree with the data achieved experimentally [15,16]. A forthcoming paper will discuss the dependence of heterogeneous and homogeneous ignition temperatures on $CH_4$–air ratio.

## 4. Catalytic conversion of methane

The numerical code, which simulates a chemical reactor containing a wire, is applied to gas-phase and catalytic oxidative coupling of methane.

The gas phase reaction scheme is taken from modelling work on homogeneous reactive flow [11,12]. The hydrocarbon mechanism used in the calculations consists of 618 elementary reactions of 54 chemical species considering reactions of the $C_1$–$C_4$ systems.

As a first example, simulation results for non-catalytic oxidative coupling during the cofeeding of methane and oxygen in an isothermal reactor ($T =$ 1023 K, $p =$ 1bar, $p_{CH_4}/p_{O_2} = 2$, $(p_{CH_4} + p_{O_2})/p_{total} = 0.7$, He dilution) are shown in Fig. 5(a). The maximum ethane selectivity occurs at a residence time of approximately 0.15 s. The methane conversion at this short residence time is still low. Hence, the yield of $C_2H_6$ hydrocarbons is very small. Ethylene is mainly formed after an induction period from ethane. The main intermediate species of CO and $CO_2$ formation is HCHO.

As a second step, the wire in the reactor is modelled with a catalytic surface which is active for methane conversion. Hereby, the heterogeneous processes are modelled by elementary reactions in addition to the gas phase mechanism. The diameter of the catalytic wire is chosen to be 1 mm and a computational domain of 1 cm in diameter is used. The same external conditions are chosen as in the non-catalytic case. Two different surface reaction mechanisms are discussed and given in Table 1.

In the first model, the catalytic effect consists of breaking a C–H bond of the $CH_4$ molecule to deliver $CH_3^{\bullet}$ radicals for further gas phase reactions. It is assumed that $10^{-4}$ of all $CH_4$ molecules striking the catalyst are dissociated on the surface. The $CH_3^{\bullet}$ radicals desorbing from the surface initiate different gas phase chain reactions leading to $CO/CO_2$ (mainly via $CH_2O/CH_3OH$) or leading to $C_2$-species (via $CH_3^{\bullet}$ recombination to $C_2H_6$). Selectivity and conversion at

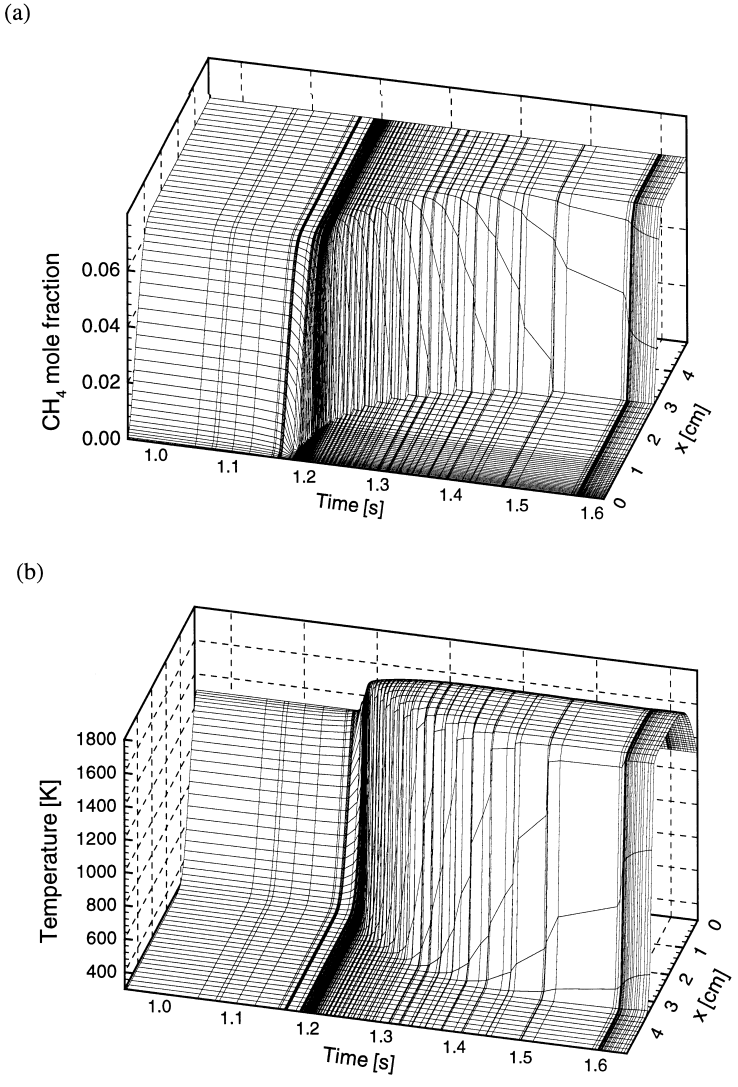


Fig. 4. Calculated methane mole fraction in the gas phase (a) and temperature (b) as a function of time and distance from the catalytic foil ($x$) during transition from heterogeneous to homogenous combustion of a lean $CH_4$–air mixture ($p_{CH_4}/p_{air} = 0.07$). The time is zero at the final increase of electric current before gas phase ignition. A different orientation of the $x$-axis is chosen in Fig. 4(b) for better visualization; the catalyst is always at $x = 0$ and shown in Fig. 1.

the outer boundary of the computational domain, 5 mm away from the catalyst, are shown in Fig. 5(b). Oxygen is consumed relatively fast, so the oxidation of methane is over after this period. However, methane conversion to ethane and finally to ethylene continues because the catalytic $CH_3^\bullet$ production is not influenced by oxygen. Aside from the rate coefficients of the catalytic reactions, the rate coefficients of the gas phase recombination $CH_3^\bullet + CH_3^\bullet \rightarrow C_2H_6$ have to be known very accurately in order to model methane conversion.

In the second model, adsorbed oxygen is a prerequisite for $CH_3^\bullet$ formation, as shown in Table 1. Hydrogen atoms (coming from $CH_4$ destruction) form water with oxygen or recombine to leave the surface as molecular hydrogen. $CH_3^\bullet$ radicals on the surface can desorb into the gas phase. Furthermore, the complete oxidation of $CH_4$ on the surface is possible. Here, a

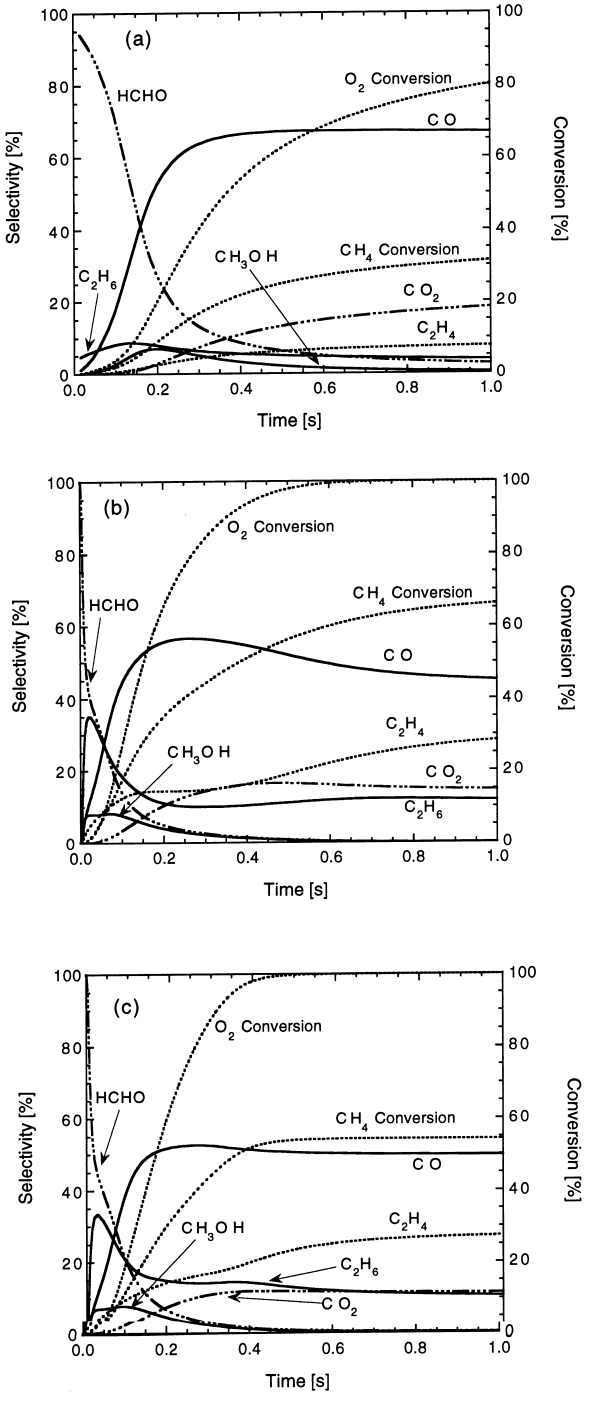


Fig. 5. Calculated conversion ($CH_4$, $O_2$) and C atom selectivity of products (CO, $CO_2$, $C_2H_4$, $C_2H_6$, HCHO, $CH_3O$) for a methane/oxygen mixture diluted by helium ($p_{CH_4}/p_{O_2} = 2$, $(p_{CH_4} + p_{O_2})/p_{total} = 0.7$, $p_{total} = 1$ bar, $T = 1023$ K) as a function of residence time in an isothermal cylindrical reactor containing a wire as shown in Fig. 1 (right). The data are taken at a distance of $r = 5$ mm away from the wire. The chemistry model includes only gas phase reactions (a), gas phase and surface reaction model 1 (b), gas phase and surface reaction model 2 (c).

Table 1
Surface reaction mechanisms used for the modelling of catalytic methane conversion

| Reaction | Implemented in model |
|---|---|
| $CH_4 + 2(s) \rightarrow CH_3(s) + H(s)$ | 1 |
| $CH_3(s) \rightarrow CH_3 + (s)$ | 1,2 |
| $2\,H(s) \rightarrow H_2 + 2\,(s)$ | 1,2 |
| $CH_4 + O(s) + (s) \rightarrow CH_3(s) + OH(s)$ | 2 |
| $H(s) + O\,(s) \rightarrow OH(s) + (s)$ | 2 |
| $H(s) + OH\,(s) \rightarrow H_2O + (s)$ | 2 |
| $OH(s) + OH(s) \rightarrow H_2O + O(s)$ | 2 |
| $O_2 + 2\,(s) \rightarrow 2\,O(s)$ | 2 |
| $CH_3(s) + (s) \rightarrow CH_2(s) + H(s)$ | 2 |
| $CH_2(s) + (s) \rightarrow CH(s) + H(s)$ | 2 |
| $CH(s) + (s) \rightarrow C(s) + H(s)$ | 2 |
| $C(s) + O(s) \rightarrow CO(s) + (s)$ | 2 |
| $CO(s) + O(s) \rightarrow CO_2 + 2(s)$ | 2 |
| $CO(s) \rightarrow CO + (s)$ | 2 |

(s) – uncovered active surface site, A(s) – species adsorbed.

competition between desorption and oxidation of $CH_3(s)$ influences selectivity. The simulation shows that the conversion process is almost terminated after oxygen is completely consumed, Fig. 5c.

The interaction of kinetics and transport processes is revealed in Fig. 6. Here, the second surface reaction model is used to simulate the catalytic conversion of a methane–oxygen mixture with $p_{CH_4}/p_{O_2} = 10$ (otherwise, the same conditions are used as described above). Ethane is formed close to the catalyst as a result of desorbing $CH_3^{\bullet}$ radicals as long as oxygen is available. In contrast to ethane, ethylene does not show strong radial gradients. Hence, ethylene is formed after ethane diffusion through the reactor.

## 5. Conclusions

The computational tools developed allow the modelling of transient processes of catalytic methane oxidation and conversion. The global behaviour of the heterogeneous reactive system can be explained by

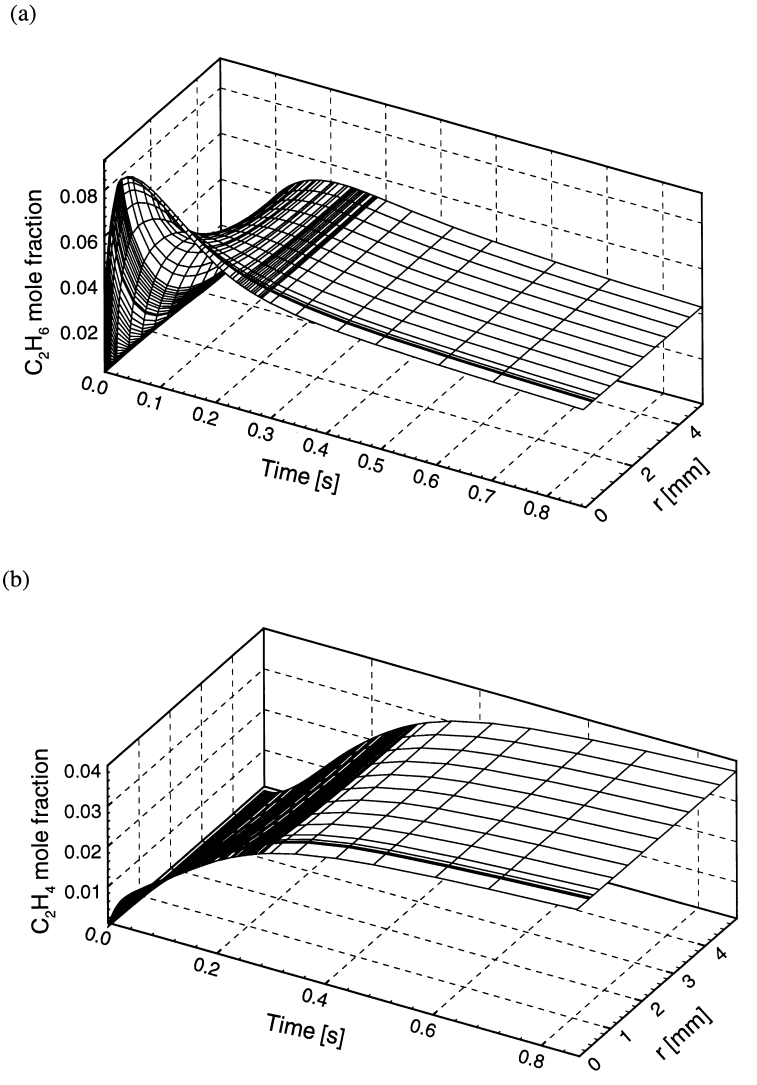


Fig. 6. Calculated ethane (a) and ethylene (b) mole fraction in the gas phase as a function of residence time and distance ($r$) from the catalyst for a methane–oxygen mixture diluted by helium ($p_{CH_4}/p_{O_2} = 10$, $(p_{CH_4} + p_{O_2})/p_{total} = 0.7$, $p_{total} = 1$ bar, $T = 1023$ K); isothermal cylindrical reactor containing a catalytic wire as shown in Fig. 1 (right); gas phase and surface reaction model 2 are used in the simulation.

elementary steps in the gas phase and at the gas–surface interface. Catalytic systems, where proper surface reaction mechanisms with the associated rate expressions are known, can be described in detail and the decisive steps can be elucidated, as was shown for the catalytic methane oxidation on platinum. Otherwise, more experimental and modelling work is recommended (especially in determining rate coefficients) to allow quantitative simulation of more complex problems, such as the oxidative coupling of methane. Inspite of that, simulations can lead to the decisive reaction channels and to a better understanding of such systems. Furthermore, parameter regions of maximum selectivity and yield can be determined.

## Acknowledgements

This work was supported by the Deutsche Forschungsgemeinschaft (DFG) within the Sonder-

forschungsbereich 359 ‘Reaktive Strömung, Diffusion und Transport’.

## References

[1] J. Warnatz, M.A. Allendorf, R.J. Kee, M.E. Coltrin, Combust. Flame 96 (1994) 393.
[2] O. Deutschmann, F. Behrendt, J. Warnatz, Catal. Today 21 (1994) 461.
[3] G. Evans, R. Greif, ASME J. Heat Transfer 109 (1987) 928.
[4] R.J. Kee, J.A. Miller, G.A. Evans, G.H. Dixon-Lewis, 22nd Symposium (Int.) on Combustion, The Combustion Institute, Pittsburgh, 1988, p. 1479.
[5] U. Maas, J. Warnatz, Combust. Flame 74 (1988) 53.
[6] G. Goyal, U. Maas, J. Warnatz, Combust. Sci. Technol. 105 (1995) 183.
[7] J. Warnatz, 22nd Symp. (Int.) on Combustion, The Combustion Institute, Pittsburgh, 1988, p. 1696.
[8] M.E. Coltrin, R.J. Kee, F.M. Rupley, SURFACE CHEMKN, Sandia National Laboratories Report SAND90-8003B, Sandia National Laboratories, Livermore, 1990.
[9] P. Deuflhard, E. Hairer, J. Zugck, Num. Math. 51 (1987) 501.
[10] F. Behrendt, O. Deutschmann, R. Schmidt, J. Warnatz, in: B.K. Warren, S.T. Oyama (Eds.), Heterogeneous Hydrocarbon Oxidation, ACS Symposium Series 638, Washington, Ch. 4, 1996, p. 48.
[11] D.L. Baulch, C.J. Cobos, R.A. Cox, C. Esser, P. Frank, Th. Just, J.A. Kerr, M.J. Pilling, J. Troe, R.W. Walker, J. Warnatz, J. Phys. Chem. Ref. Data 21 (1992) 411.
[12] V. Karbach, J. Warnatz, publication in preparation.
[13] D.A. Hickman, L.D. Schmidt, AIChE J. 39 (1993) 1164.
[14] O. Deutschmann, R. Schmidt, F. Behrendt, J. Warnatz, 26th Symposium (Int.) On Combustion, The Combustion Institute, Pittsburgh, 1996, p. 1747.
[15] G. Veser, L.D. Schmidt, AIChE J. 42 (1996) 1077.
[16] R. Schmidt, Dissertation, Fakultät Chemie der Ruprecht-Karls-Universität Heidelberg, 1998.